2021 IEEE 32nd Annual International Symposium on Personal, Indoor and Mobile Radio Communications (PIMRC) | 978-1-7281-7586-7/21/$31.00 ©2021 IEEE | DOI: 10.1109/PIMRC50174.2021.9569532

# Analysing the 3GPP Spatial Consistency Procedure Through Channel Measurements

William Sloane[†‡], Mansoor Shafi[*], Camillo Gentile[§], Graeme Woodward[†],
Philippa Martin[‡], Pan Tang[¶], Jianhua Zhang[¶] Chiehping Lai[§]
[†]Wireless Research Centre, University of Canterbury, Christchurch, New Zealand
[‡]Electrical and Computer Engineering, University of Canterbury, Christchurch, New Zealand
[*]Spark New Zealand, Wellington New Zealand
[§]Wireless Networks Division, National Institute of Standards and Technology, Gaithersburg, MD
[¶]State Key Lab of Networking and Switching Technology, Beijing University of Posts and Telecommunications
william.sloane@pg.canterbury.ac.nz, (philippa.martin, graeme.woodward)@canterbury.ac.nz,
(camillo.gentile, chiehping.lai)@nist.gov, mansoor.shafi@spark.co.nz, (jhzhang, tangpan27)@bupt.edu.cn

***Abstract*—Millimeter-wave channel measurements for a meeting room, lecture room and open plan office floor were used to analyse and model the spatial consistency of channel clusters. Particularly, how the angles of arrival and delays of extracted multi-path components in each cluster varied with small changes in receiver location. We extended the KPowerMeans algorithm, for classifying captured multi-path components into clusters from the delay/angular domains, to include the location domain to allow the spatial consistency of the clusters between locations to be analysed. The observed spatial consistency in measurements was then used to validate whether the 3GPP spatial consistency procedure (3GPP SC-I) reflects real world spatial consistency. The 3GPP spatial consistency procedure for ensuring spatial consistency of cluster parameters during mobile user simulations was then applied for each environment, allowing for comparison between the 'predicted' cluster parameters and the measured cluster parameters. The 3GPP model/procedure showed a good fit for all environments but highlighted the impact of the environment on the amount of accuracy of the procedure.**

***Index Terms*—Millimeter-Wave, Spatial Consistency, 3GPP, Clusters, Channel Modelling, 5G**

## I. Introduction

Characterisation of Millimeter-wave (mmWave) channels is important to allow for simulations of 5G radio systems that accurately represent real world behaviour. To date a wide range of mmWave models have been produced from a variety of measurement campaigns at different frequencies and environments, such as ITU-R M.2412 by the International Telecommunication Union (ITU) [1] and TR 38.901 V16 by the 3rd Generation Partnership Project (3GPP) [2]. These focus on capturing the large scale and small scale fading properties of channels between 0.5 and 100 GHz. As mmWave channels have significantly different propagation characteristics to microwave channels, several new modelling components such as Spatial Consistency (SC), Blockages, Large Antenna Arrays and Oxygen Absorption have been identified as mandatory requirements for mmWave channel models by the ITU [1]. In this paper we focus on analysing SC.

3GPP TR 38.901 and ITU-R M.2412 model a multipath channel using clusters, where multi-path components (MPCs) arrive at the receiver in groups with similar delay and angular characteristics. Specifically, N clusters with 20 rays per cluster, where the number of clusters (N) is dependent on the type of simulated environment. These clusters are a result of the environment and geometry between transmitter (TX) and receiver (RX), particularly scattering objects, reflecting objects and the direct path. SC is the concept that when the RX changes position slightly, the delay and angular characteristics of the MPCs within each cluster will gradually change. SC can be formally defined as ensuring that in simulation the angles of arrival (AOAs), angle of departure (AODs) and delays of MPCs within each cluster smoothly evolve for small changes in user position. Previous drop based models for microwave and mmWave channels do not allow for the temporal simulation of beamforming algorithms, where for a mobile user simulation, these AOAs, AODs and delays are generated independently, with no correlation to the previous parameters which does not happen in practice. To ensure mmWave model simulations for a mobile user are spatially consistent, the 3GPP and the ITU have proposed a SC procedure ('SC-I') which updates the AOAs, AODs, and delays of MPCs within each cluster, as a user travels along a path [1] [2]. This is based on early work by Wang et al. [3], where a simple linear approximation process was proposed to update cluster AOAs and delays, as the receiver/user moves along a known path. The initial cluster MPCs and their AOAs, AODs and delays are generated at $t_k = 0$, then at $t_k = t_k + \Delta t$ the cluster AOAs, AODs, delays and UE bearing at $t_{k-1}$ are used to generate the new cluster parameters. This ensures a smooth evolution of cluster parameters, as a user moves along a track, for simulated scenarios.

The majority of research on SC to date has focused on simulating spatially consistent models using the procedures defined by the 3GPP and ITU. In [4] and [5], the evolution of cluster AOAs and delays for a mobile user scenario with and without SC are evaluated. Similarly [6] compares the beamforming performance for a mobile user with and without SC. There is a lack of literature which evaluates and models the SC of individual clusters from channel measurements, particularly for indoor environments. In [7], Dai et al. use

outdoor channel measurements to validate the SC feature of the quasi-deterministic radio channel generator (QuaDRiGa) by comparing channel realisations from simulation and measurements using covariance matrices. However, this does not analyse the 'SC-I' procedure, instead it focuses on the sum-of-sinusoids method proposed by the same authors to ensure SC.

In this paper we use previously extracted MPCs from three indoor mmWave measurement campaigns to model the SC of channel clusters for a meeting room (MR) (mesurements by Zhan et al. [8]), lecture room (LR) (measurements by NIST [9]) and large open plan office floor (OF) (measurements by Tang et al. [10]). For each environment we utilise a clustering process to determine the number of clusters throughout the channel and classify the extracted MPCs into clusters. We then demonstrate the SC of clusters from position to position and highlight key differences in the observed SC and correlation distance between the different environments. As our novel contribution, for each environment we use the 3GPP model to predict the evolution of each cluster's MPCs based on the initial AOAs, AODs and delays. We then compare the predicted cluster AOAs, AODs and delays to the measured to validate the model.

The contributions of this paper are:

- Modelling of 3GPP style Large Scale Parameters (LSPs) for the lecture room channel using the extracted MPCs. We then compare these to previously extracted LSPs for the office floor and meeting room channels to highlight the difference in environments.
- Clustering of the extracted MPCs for each environment. An appropriate clustering process is chosen, the optimal number of clusters identified, and the measured MPCs classified into clusters. We then model the SC of cluster AOAs, AODs and delays.
- Comparison of 'predicted' vs measured/observed SC. Using the observed cluster evolution, we use the 3GPP SC procedure to estimate the cluster AOAs, AODs and delays and compare these to the measured values.

The rest of the paper is as follows. Section II summarises the three indoor environments and their respective measurement campaigns. Section III presents the LSPs characterising the three channels and describes the clustering process used to enable modelling of SC. Section IV, presents the measured and predicted SC and analyses the key differences. Section V summarises the paper.

## II. Measurement Campaigns and Data Processing

Fig 1. shows the layout of the three environments and the simulated RX track used to evaluate the 3GPP SC model/procedure. Table I. summarises the key measurement and environmental parameters for each environment.

### A. Lecture Room - NIST Campus, Boulder, Colorado

Channel measurements at 60 GHz were undertaken in a lecture room populated with chairs and tables as part of an extensive mmWave channel campaign by the National Institute of Standards and Technology (NIST). The measurement and MPC extraction technique is described in detail in [9], the key details relevant to this paper are summarised below. A stationary TX and mobile RX mounted on a robot captured the channel at measurement locations approximately 0.25-1m apart as the RX robot followed a rectangular path around the room. A bi-directional channel sounder with a 0.5 ns delay resolution with electronically switched antenna arrays and a 180° and 360° field of view (FOV) at the TX and RX respectively was used to capture the complex impulse response (CIR) at each RX location. Using the captured CIRs, NIST then used their super resolution space-alternating generalized expectation-maximization (SAGE) algorithm to extract the channel MPCs in the delay, AOA, AOD, zenith angle of arrival (ZOA) and zenith angle of departure (ZOD) for each measurement location.

TABLE I: Measurement and Spatial Consistency Parameters

| | LR [9] | OF [10] | MR [8] |
|---|---|---|---|
| Frequency (GHz) | 60 | 28 | 28 |
| Room Dimensions (m) | 10x19 | 50x20 | 11x7 |
| Number of RX Locations | 82 | 7 | 12 |
| RX Distance Travelled (m) | 36 | 35 | 20 |

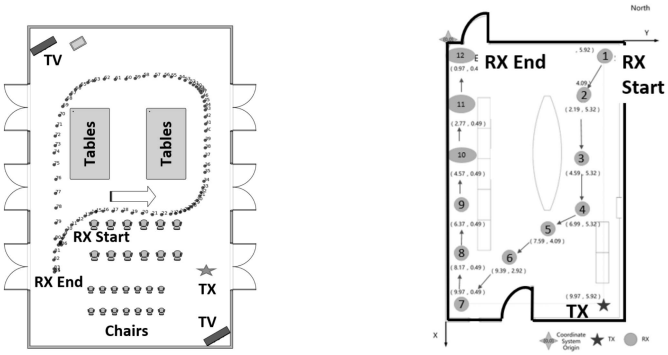


(a) Lecture Room [9]. (b) Meeting Room [8].

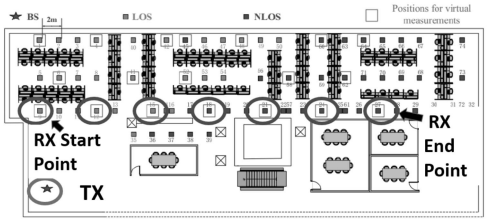


(c) Office Floor [10].

Fig. 1: Measurement environments with simulated RX paths.

### B. Large Open Plan Indoor Office Floor - Wellington, NZ

Channel measurements were taken and processed by Tang et al. [10], the process is summarised below. Channel measurements were taken at 28 GHz and MPCs extracted to facilitate the modelling of 3GPP style channel parameters in the same paper. The measurement environment was a large open plan office floor with rows of desks, meeting rooms and walkways.

Measurement locations were more separated than the lecture room dataset with locations ranging from 2-4 m apart. For the purpose of modelling SC we simulate a user walking next to the rows of desks as shown in Fig 1c. At each receiver location a directional horn antenna was used and electronically rotated to achieve a 360° FOV, a omni-directional antenna was used at the TX. To obtain angle of departure information the TX and RX antennas were then interchanged. Using the SAGE algorithm MPCs were then extracted in the AOA, AOD, ZOA and ZOD domains with a 5° angular resolution at each measurement location.

### C. Small Meeting Room - BUPT Campus, Beijing, China

These measurements were taken and processed by Zhan et al. [8], the process is summarised below. The measurements were taken in a small meeting room with table and chairs on the BUPT campus at 28 GHz, using a similar method to that used for the office floor measurements. Similarly to the office floor measurements a omni-directional antenna was used at the TX and a horn antenna was rotated at the RX to achieve a 360° FOV. Unlike the office measurements, the TX and RX antennas were not interchanged, therefore, no angle of departure information is available for these measurements.

## III. Large Scale Parameter Modelling and Channel Clustering

### A. Large Scale Parameters

For each environment we present the following large scale parameters as specified by 3GPP TR 38.901 [2], to highlight the differences between the three indoor environments: RMS delay spread (RMS DS); K-Factor; Path Loss (PL); and RMS Angular Spread (RMS AS). Large scale parameters for the office floor and meeting room have been extracted as part of previous publications in [10] and [8], respectively. In this study we extract these for the NIST lecture room.

A similar process to that described in [10] was used to model the LSPs for the lecture room channel. Using the MPCs captured at each location the RMS DS, K-Factor and RMS AS were calculated for each RX location. For each parameter the calculated values for each RX location were combined to form an overall dataset which was then fitted with a log-normal distribution per the 3GPP model, using minimum mean square error estimation. For the path loss parameters the close in (CI) model was fitted [2], where $n$ is the path loss exponent (PLE) and $X_{CI}$ is the overall shadowing.

The extracted large scale parameters for each of the three environments are shown below in Table II. The 3GPP indoor hotspot parameters for both 28 (3GPP 28) and 60 GHz (3GPP 60) are provided for comparison [2]. It should be noted that 3GPP defines an indoor hotspot as a 120 x 50 m office floor. The mean and standard deviation for the fitted log-normal distribution are represented by $\mu$ and $\sigma$ respectively.

When analysing the large scale fading characteristics of each environment in Table II., we see the meeting room and lecture room have significantly lower delay spreads than the office floor and 3GPP indoor hotspot. The enclosed environment results in more reflected paths which also results in lower K factor values highlighting a less dominant direct path. We also see less angular dispersion in the meeting room and lecture room environments. The higher path loss for the lecture room is likely a result of the higher frequency. In summary, the three different environments all display similar characteristics to the 3GPP indoor hotspot values but small differences highlight the environmental and frequency sensitivity of the mmWave.

TABLE II: Large Scale Parameters

| | | LR | OF | MR | 3GPP 28 | 3GPP 60 |
|---|---|---|---|---|---|---|
| RMS DS | $\mu$ | -7.92 | -7.9 | -8.02 | -7.70 | -7.7 |
| | $\sigma$ | 0.08 | 0.24 | 0.18 | 0.10 | 0.10 |
| K-Factor | $\mu$ | 5.20 | 6.15 | 3.24 | 7 | 7 |
| | $\sigma$ | 4.30 | 3.44 | 3.20 | 4 | 4 |
| Path Loss | $n$ | 1.87 | 1.45 | 1.81 | 1.73 | 1.73 |
| | $X_{CI}$ | 2.74 | 1.70 | 1.85 | 3.00 | 3.00 |
| RMS ASA | $\mu$ | 0.68 | 1.15 | 0.67 | 1.43 | 1.37 |
| | $\sigma$ | 0.02 | 0.29 | 0.02 | 0.23 | 0.21 |
| RMS ASD | $\mu$ | 0.71 | 1.07 | NA | 1.60 | 1.60 |
| | $\sigma$ | 0.06 | 0.28 | NA | 0.18 | 0.18 |

### B. Clustering Process

Two approaches to clustering the measured MPCs were considered. The traditional approach to modelling the evolution of clusters across RX locations is to cluster them independently at each RX location based on the 3GPP model, where MPCs are classified into clusters using their AOAs, AODs and delays. One disadvantage of this approach is measurement anomalies can significantly skew the location of the cluster centroids which results in a lack of apparent SC between RX locations. As each RX location is clustered independently, even if the captured MPCs are very similar between successive locations, slight differences in the measured MPCs can cause the cluster centroids to be in completely different positions. This makes observing SC difficult.

The second approach [11], imposes SC, by assuming cluster centroids will be spatially consistent between locations. The clustering algorithm is extended to the location domain which enables delay/angle clusters to be linked between locations, hence imposing SC. There are several advantages of this approach. Cluster birth and death is easily identifiable, as clusters are linked over the location domain. With the first method it is hard to distinguish whether a lack of spatial consistency is a result of cluster birth and death or measurement error. This method also allows for all MPCs within a cluster to be displayed visually, as opposed to the cluster centroid only.

To provide the best visualisation of SC, the second clustering process was used where SC is imposed by extending the clustering to the location domain. For the lecture room measurements, 5 dimensions were used to fit the clusters (AOA, AOD, ZOA, ZOD and delay). For the office floor measurements 4 dimensions were used (AOA, AOD, ZOA, ZOD). For the meeting room measurements no angle of departure information was measured hence 2 dimensions were used (AOA, ZOA). The clustering process (used for each of the 3 sets of measurements) is based on the KPowerMeans algorithm

described in [12] and [13]. Firstly, the MPCs from each RX location are combined into one dataset, with MPCs with a path gain less than 13 dB above the noise floor filtered out. Each MPC is given an additional dimension representing the RX location at which it was measured. The cluster centroids are then initialised as described in [13] and the KPowerMeans algorithm assigns each MPC to the cluster which minimises the multi-component distance (MCD) in all dimensions. The cluster centroids are then recalculated after each iteration. The KPowerMeans is run for a range of K values (number of clusters to be fitted) and the 'CombinedValidation' method used to determine which K value produces the most optimal cluster classification. With the cluster classification for the optimal K value, the 'ShapePrune' algorithm is used to remove significant outliers from clusters.

Simple ray-tracing was used to further verify the final cluster classification for each environment. The final cluster numbers for each environment is presented in Table III with the 3GPP cluster numbers provided for comparison. It should be noted that the 3GPP model assumes a constant number of clusters throughout a channel, whereas our approach accounts for the birth and death of clusters. We note the meeting room and lecture room have fewer clusters than the 3GPP environment, it is likely this is a result of the smaller and enclosed rooms.

TABLE III: Cluster Numbers

| | Lecture Room | Office Floor | Meeting Room | 3GPP InH |
|---|---|---|---|---|
| K | 10 | 11 | 9 | 15 |

## IV. Spatially Consistent Modelling

### *A. Observed Spatial Consistency of Clusters from Measurements*

Using the described location based clustering algorithm we analyse the SC of the clusters along the RX path for each of the three environments. We visualise the evolution of the clusters by displaying the clustered MPCs in 3 dimensions with the Z axis (vertical axis) representing the RX location (along the RX path). As the MPCs captured in each environment have different extracted dimensions, with the X and Y axes we display the delays and AOAs, AOAs and ZOAs, AOAs and AODs of the MPCs for the lecture room, meeting room and office floor environments respectively, to best highlight the SC of clusters. These are shown in Fig 2., where MPCs in each cluster are represented by a different marker symbol and colour.

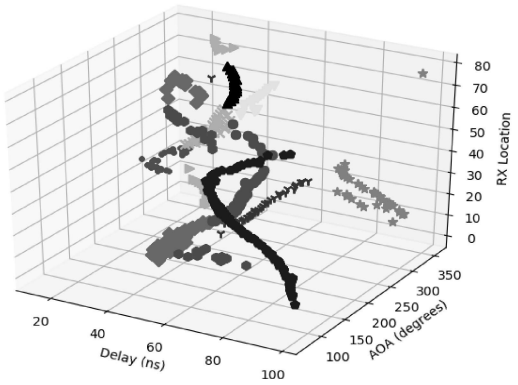


(a) Lecture Room

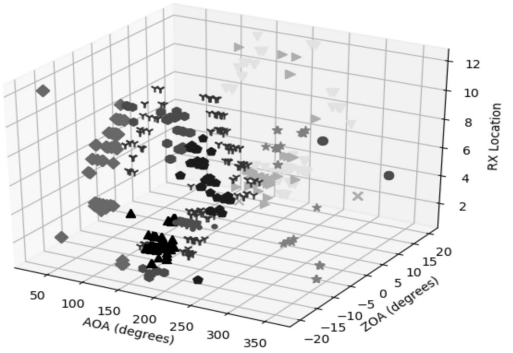


(b) Meeting Room

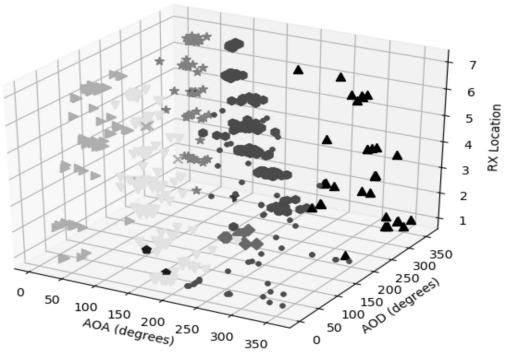


(c) Indoor Office Floor

Fig. 2: Observed SC of Clustered MPCs

*1) Analysis:* We see that for all three environments, the AOAs, ZOAs and delays for each cluster gradually change for each RX location indicating spatial consistency. Some notable differences in how the clusters evolve can be mapped to differences in the RX paths between the three environments. For the office floor channel (Fig 2c.) where the RX moves in a straight line we see the clusters evolve gradually in a linear fashion, indicating high levels of SC. In both the meeting room (Fig 2b.) and lecture room (Fig 2a.) channels the RX turns multiple corners, these are reflected in the observed evolution of the cluster AOAs and delays. The evolution appears piecewise, where the discontinuities map to the RX changing direction. While the meeting room track starts and finishes at different locations, the lecture room RX track begins and finishes in very similar locations which intuitively means the channel at these locations should be spatially consistent. This is evident in Fig 2a. (lecture room), where some clusters are observed at RX locations 70-80 and RX locations 1-10 but not in between. Cluster birth and death is particularly evident

in the lecture room channel where clusters are only visible between some locations.

### B. Evaluating 3GPP Spatial Consistency Procedure-I

In this section we determine whether the 3GPP/ITU SC Procedure-I [1] [2], for updating cluster AOAs and delays based on the RX direction of travel, is representative of the SC observed in the dataset. To do this, the AOAs, AODs and delays of the clusters identified from the measurements at the first RX location (for each environment) were updated by the procedure at intervals that match where the actual measurements were taken to allow for direct comparison. In simulation the procedure is applied to all MPCs, however, we apply it to the cluster centroid (mean of MPCs within a cluster) for each cluster, as it allows for the best visual comparison and validation.

The process used to generate cluster AOAs and delays for each environment is outlined below in Algorithm 1.

**Algorithm 1:** Iterative procedure for updating cluster AOAs and delays

For each cluster when it is first observed, identify the cluster centroid's AOA, AOD and delay from the measured/observed clusters.
**for** *all subsequent RX locations* **do**
  Calculate RX bearing relative to TX;
  Update the centroid's AOA, AOD and delay using (1)-(9) defined below [1, eq. (7.2.1 - 7.2.9)].
**end**

The 3GPP procedure uses linear approximation equations to predict the evolution of the cluster AOAs, ZOAs and delays, where the next AOA/ZOA/delay is the previous AOA/ZOA/delay plus some slope which represents the rate of change of the angle as a result of the RX moving location [1]. The AOA for the next location is given by

$$\phi_{n,AOA}(t_{k-1}+\Delta t) = \phi_{n,AOA}(t_{k-1}) - \Delta_d S_{AOA}, \quad (1)$$

where

$$S_{AOA} = \frac{S_{T1} - S_{T2}}{S_B}, \quad (2)$$

$$S_{T1} = (sin(\theta_v)cos(\phi_{n,AOA}(t_{k-1})), \quad (3)$$

$$S_{T2} = (cos(\theta_v)sin(\phi_{n,AOA}(t_{k-1})), \quad (4)$$

$$S_B = \tau_{(t_{k-1})}sin(\theta_{ZOA}(t_{k-1})). \quad (5)$$

The ZOA is given by

$$\theta_{n,ZOA}(t_{k-1}+\Delta t) = \theta_{n,ZOA}(t_{k-1}) - \Delta_d S_{ZOA}, \quad (6)$$

$$S_{ZOA} = \frac{\boldsymbol{r}_{rx,n}(t_{k-1})^T \boldsymbol{v}(t_{k-1})}{\tau_{(t_{k-1})}c}\Delta_d, \quad (7)$$

$$\boldsymbol{r}_{rx,n} = \begin{bmatrix} sin(\theta_{ZOA}(t_{k-1}))cos(\phi_{n,AOA}(t_{k-1})) \\ sin(\theta_{ZOA}(t_{k-1}))sin(\phi_{n,AOA}(t_{k-1})) \\ cos(\theta_{ZOA}(t_{k-1})) \end{bmatrix}. \quad (8)$$

The delay is given by

$$\tau_n(t_{k-1}+\Delta t) = \tau_n(t_{k-1}) - \frac{\boldsymbol{r}_{rx,n}(t_{k-1})^T \boldsymbol{v}(t_{k-1})}{c}\Delta_d. \quad (9)$$

For all equations, $\phi_{n,AOA}$, $\theta_{n,ZOA}$, and $\tau_n$ represent the AOA, ZOA, and delay for the nth cluster centroid respectively, $\theta_v$ represents the direction of travel of the RX relative to the TX and $\boldsymbol{v}(tk-1)$ is the RX velocity vector. The RX paths shown for each environment in Fig 1. were used as the 'simulated' RX path. A key parameter in using this procedure is the 'correlation distance', this defines the distance in which the procedure should be used before new 'measured data' is obtained. The 3GPP and ITU set this as 15m for indoor hotspots. For our simulations, we use the procedure for the entirety of the RX path and then estimate the true correlation distance for comparison in our analysis.

Fig 3. shows the AOAs of the 'predicted' cluster centroids overlayed on AOAs of the clustered measured MPCs for each environment. Fig 4. shows the delays of the predicted cluster centroids and delays of the clustered measured MPCs for the lecture room channel. For clarity, we only show the predictions for the most significant clusters to avoid clutter on the plots. It is noticeable that for the office floor and meeting room clusters, several clusters have very similar AOAs, but are different in other domains, therefore for the AOA plots several clusters appear overlayed on top of each other.

*1) Analysis:* We see that for all three environments, the predicted cluster AOAs and delays show a good fit to the cluster AOAs and delays extracted from measurements. Examining the measured cluster delays for the lecture room channel, we see that there are 'turning points' where the delay changes from increasing to decreasing or vice versa. These can be mapped to the RX robot turning a corner and is predicted by the 3GPP procedure. With clusters that undergo cluster birth and death we see the 3GPP procedure accurately predicts the cluster evolution when it is observable. Focusing on the purple cluster in Fig 3a. (lecture room), we see from RX location 10 to 42 the cluster is observed and accurately predicted. When estimating a suitable correlation distance for the lecture room, the differing correlation distances of individual clusters must be considered. As some clusters are only visible over ten or less RX locations (5-10 m), a suitable correlation distance would be 10 m or less. This would ensure that the death or birth of a cluster is quickly picked up.

Examining the predicted AOAs for the meeting room we see that the trend matches that of the observed AOAs, but the observed AOAs increase and decrease more than what is predicted. This may be a result of the smaller room size resulting in significantly more variation between RX locations. To accurately predict the evolution, a correlation distance of 5 m or less is necessary. Future work will utilise beamforming with both the predicted and measured cluster parameters to determine the significance of the difference between the measured and predicted parameters.

For the office floor despite the RX travelling 35 m from start to finish, we see clear linear evolution of the AOAs for each

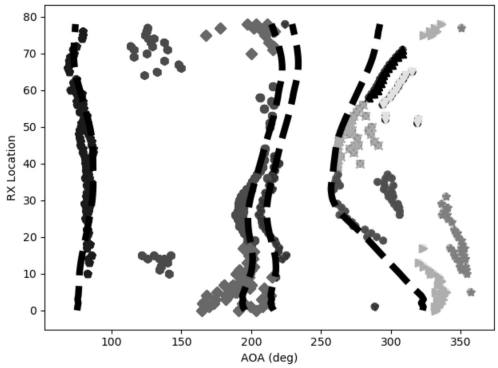


(a) Lecture Room.

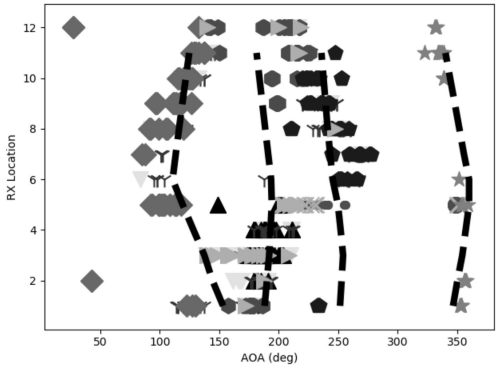


(b) Meeting Room.

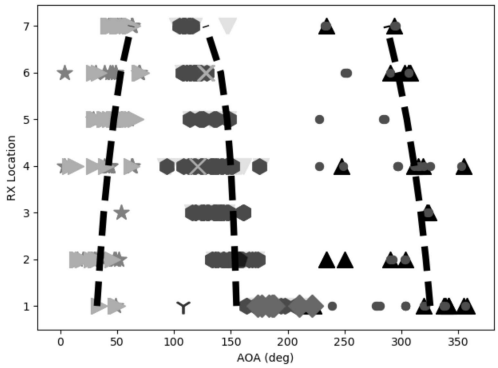


(c) Office Floor.

Fig. 3: AOAs of clustered measured MPCs, with AOAs of predicted cluster centroids shown (dashed lines). For clarity we only show the predictions for the most significant clusters.

cluster predicted by the 3GPP model. This shows that for a larger indoor environment, particularly if the RX is travelling a straight line, the correlation distance is likely to be atleast the 3GPP specified 15 m. For this environment we estimate a conservative correlation distance of 20 m.

## V. Conclusion

The 3GPP procedure for evolving cluster parameters in a spatially consistent manner accurately matches the observed evolution of cluster parameters from measurements taken in three different indoor environments. While there are small deviations between the observed and predicted, the general trend of the observed cluster evolution is captured by the model, particularly when the RX changes direction significantly. Our results also show that the appropriate correlation distance is highly dependent on the RX path and environment, with the larger office floor having a significantly higher correlation distance than the smaller meeting and lecture rooms.

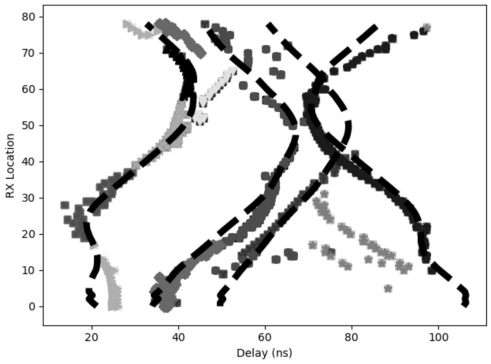


Fig. 4: Predicted cluster centroid delays (dashed line) for lecture room.

## References

[1] "ITU-R M.2412-0. Guidelines for evaluation of radio interface technologies for IMT-2020," International Telecommunication Union, Technical, Oct. 2017.

[2] "ETSI TR 138 901 V14.3.0 5G; Study on channel model for frequencies from 0.5 to 100GHz," 3GPP, Industry Standard, Jan. 2018.

[3] Y. Wang *et al.*, "An extension of spatial channel model with spatial consistency," in *2016 IEEE 84th Vehicular Technology Conference (VTC-Fall)*, Sep. 2016, pp. 1–5.

[4] Y. Guangzhong *et al.*, "The method to implement 5G channel model with spatial consistency," in *IEEE/CIC International Conference on Communications in China (ICCC)*, Aug. 2018.

[5] M. Shafi *et al.*, "Microwave vs. millimeter-wave propagation channels: Key differences and impact on 5G cellular systems," *IEEE Communications Magazine*, vol. 56, no. 12, pp. 14–20, Dec. 2018.

[6] H. Tataria and F. Tufvesson, "Impact of spatially consistent channels on digital beamforming for millimeter-wave systems," in *14th European Conference on Antennas and Propagation*, Mar. 2020.

[7] S. Dai *et al.*, "Spatial consistency validation on massive SIMO covariance matrices in the geometry-based stochastic channel model QuaDRiGa," in *WSA 2020; 24th International ITG Workshop on Smart Antennas*, 2020, pp. 1–6.

[8] J. Zhan *et al.*, "Comparative channel study of ray tracing and measurement for an indoor scenario at 28 GHz," in *12th European Conference on Antennas and Propagation (EuCAP 2018)*, Apr. 2018, pp. 1–5.

[9] C. Lai *et al.*, "Methodology for multipath-component tracking in millimeter-wave channel modeling," *IEEE Transactions on Antennas and Propagation*, vol. 67, no. 3, pp. 1826–1836, Mar. 2019.

[10] P. Tang *et al.*, "Millimeter wave channel measurements and modelling in an indoor hotspot scenario at 28 GHz," in *2018 IEEE 88th Vehicular Technology Conference (VTC-Fall)*, Aug. 2018, pp. 1–5.

[11] N. Varshney *et al.*, "Quasi-deterministic channel propagation model for an urban environment at 28 GHz," *Under revision in IEEE antennas and Wireless Propagation Letters*, March 2021.

[12] N. Czink *et al.*, "A framework for automatic clustering of parametric MIMO channel data including path powers," in *IEEE Vehicular Technology Conference*.

[13] P. Tang *et al.*, "Clustering in 3D MIMO channel: Measurement-based results and improvements," in *2015 IEEE 82nd Vehicular Technology Conference (VTC2015-Fall)*, Sep. 2015, pp. 1–6.